Brazilian Journal of Geophysics (2022) 40(Suppl. 1): 1–14
Brazilian Geophysical Society
ISSN 2764-8044
DOI: 10.22564/brjg.v40i5.2148

CHRONOLOGICAL STUDY OF SEDIMENTS FROM ALAMBARI RIVER, SÃO JOSÉ DOS CAMPOS, SÃO PAULO STATE, BRAZIL: IMPACTS OF INDUSTRIAL AND OIL REFINERY ACTIVITIES

Daniel Marcos Bonotto * and João Pedro Massari

[1]Universidade Estadual Paulista - UNESP, Instituto de Geociências e Ciências Exatas - IGCE, Rio Claro, SP, Brazil

*Corresponding author email: daniel.bonotto@unesp.br

ABSTRACT. Several studies in Nuclear Geophysics have adopted the ^{210}Pb chronological method to determine sedimentation rates in hydrographic basins. In this paper, such technique was utilized to investigate sediments collected from the Alambari River, located in the vicinity of the Henrique Lage Refinery (Revap - Petrobras), in the municipality of São José dos Campos, São Paulo State, Brazil. This study was carried out in order to observe the potential anthropic influences of the refinery on the Alambari River sediments. For the collected sediments, analysis including loss on ignition (LOI), grain size, chemical composition, and sedimentation rates/sediment age were carried out, in this case, adopting the ^{210}Pb Constant Rate of Supply (CRS) model. The average sedimentation rate varied between 0.363 g/cm^2.year and 1.68 g/cm^2.year. Silica was identified as the main constituent in all three sediment cores analyzed in this study, with average concentrations of 41.63-82.58% and was correlated inversely with aluminum, iron and titanium, among other oxides. The X-ray fluorescence spectrometry also allowed identifying the presence of elements that could be associated with petroleum and its derivatives, such as palladium, nickel and vanadium, possibly indicating the contamination of sediments of the Alambari River by effluents or leaks due to the refinery's activities.

Keywords: environmental contamination, Pb-210 chronological method, sedimentation rate, oil refinery, Alambari River.

INTRODUCTION

The environmental issue is progressively more present in the urban perimeters. Environmental problems linked to geology also occur in certain regions. However, anthropic action is often responsible for accelerating some natural geological processes, in addition to being responsible for much of the contamination in soils, subsoils and drainages, which can be harmful to the environment and population.

Among the substances that enter aquatic environments, heavy metals constitute a group of elements whose abundance has been widely studied, due to their toxicity and because of their natural and anthropogenic origin (French, 1993). The ^{210}Pb dating method can be applied to measure the rate of sediment accumulation in several environments (Sharma et al., 1987). When ^{210}Pb enters a river, lake or ocean, it ends up being deposited on the bottom through sedimentation and chemical exchange processes, joining to the sediment layers. However, in addition to have ^{210}Pb originating from the atmosphere, the sediment also contains ^{210}Pb generated by the ^{226}Ra decay.

In the environment, ^{210}Pb occurs as one of the radioisotopes in the natural decay series of ^{238}U. The imbalance between ^{210}Pb and ^{226}Ra (half-life of 1602 years) occurs through the release of part of ^{222}Rn (half-life of 3.82 days), which escapes from the soil and diffuses into the atmosphere (Cazotti et al., 2006). A portion of the ^{222}Rn formed by ^{226}Ra is released through the soil interstices and diffuses into the atmosphere, where it decays forming a sequence of several short half-lived nuclides, until the formation of the relatively long half-lived ^{210}Pb (22.26 years), which is called ^{210}Pb$_{exc}$, i.e., in excess (Cazotti et al., 2006).

The ^{210}Pb generated and incorporated into the sediments is very reactive and quickly associates with the particles, precipitating later on the surface. This makes it useful for studies of inflows and processes that determine the distribution of reactive elements in sediments, such as heavy metals, thus, allowing estimating sedimentation rates and calculating the age of specific strata in the sediment column. The corresponding timescale is equivalent to 5-7 times its half-life, that is, the last 120-150 years, during which the industries of many urban areas were developed. Therefore, by means of appropriate experiments, contaminants present in different sediment cores may be identified and their deposition age determined as well. This is also valid for constituents associated with organic compounds possibly arising from the oil refining process. Therefore, the target of this study is an area linked to the development of activities devoted to the petroleum refinement, which is related to environmental concerns due to possible contamination of the environment and human proximity to polluting substances present in the several industrial stages involved.

In a portion of the Paraíba do Sul River basin, more specifically in the region of São José dos Campos city, São Paulo State, Brazil, problems of leaks and environmental contamination from Henrique Lage Refinery (Revap) were announced several times. The Revap construction started in February 1974 and, in this sense, it is highly relevant to get information about the chronology of the Alambari River sediments accompanied by their chemical composition. This is because the sedimentation rate and age of the sediments are important descriptive parameters of the hydrographic basins, allowing, in parallel, following the evolution of the concentration levels of contaminants in the aquatic systems.

Thus, the main objective of this paper consisted in determining the age of the sediments and the sedimentation rate in Alambari River in São José dos Campos, using the dating method of the Constant Rate of ^{210}Pb Supply (CRS). Its use allowed establishing the chronology of the sedimentary layers, permitting to correlate the sedimentation rates with some parameters and to monitor historical changes in the concentrations of different constituents along the cores.

STUDY AREA

The study area of this investigation is located in the eastern portion of the State of São Paulo, Brazil, and corresponds to an area framed in the territory of the municipality of São José dos Campos. It is inserted in the hydrographic basin of the Paraíba do Sul River, being drained by the river Paraíba do Sul and its tributaries. Next to the research area it is located the oil refinery Revap, which is a site susceptible to the release of contaminants.

Also, the area is situated along the Alambari River in São José dos Campos (Figure 1). The collection points for sediment core samples can be accessed by roads and regions located close to Revap (Figure 1). The first sampling point can be accessed through the São José dos Campos neighborhood and is located in Alambari Park, next to Hanna Youssef Chabchoul street. The second sampling point can be accessed by the side of *Presidente Dutra* Highway, opposite to the *Vila Tatetuba* neighborhood, on an undeveloped land near Revap.

Furthermore, the study area is located within the Taubaté Basin in the southeastern region of Brazil, east of the São Paulo State. Geomorphologically, the study site is located in the Paraíba do Sul River Valley between *Serra da Mantiqueira* and *Serra do Mar*. The Taubaté Basin has an elongated shape in the ENE-WSW direction with a width of 20 km and an approximate length of 170 km, with an area of about 3,200 km^2 (Vidal et al., 2004; Riccomini et al., 2004).

The Taubaté Basin belongs to a set of Cenozoic Taphrogenic Basins, which is called by Riccomini (1989) as the Continental Rift of Southeast Brazil (RCSB), a tectonic feature of Cenozoic age, which is located between the cities of Curitiba (Paraná State) and Barra de São João (Rio de Janeiro State). These taphrogenic basins (Taubaté, São Paulo, Curitiba, Resende and Volta Redonda) constitute a single elongated depression in the ENE-WSW direction and accompany the main basement structures in the region (Riccomini et al., 2004).

The deposition of sediments in this basin is typically continental and its filling can be separated into two phases. The first one is linked to a syn-tectonic phase to the rift, with deposition of sediments from the Taubaté Group, composed by the Resende, Tremembé, and São Paulo formations. The second one is related to a later phase of diastrophic tectonics, with the deposition of the Pindamonhangaba Formation and alluvial and colluvial deposits.

SAMPLING

The collection of samples for this research took place in 2020 within the urban perimeter of São José dos Campos. In order to carry out this work, three sediment cores were collected in the drainage called Alambari River, with one sediment core collected at point 1 and two sediment cores collected at point 2 (Figure 1). The sampling sites comprised collections conducted upstream (core 1) and downstream (cores 2.1 and 2.2) of Revap.

The sediment collection points were chosen based on the possible anthropogenic anomalies in the composition of the sediments, as indicated by Bonotto et al. (2005) and Bonotto and Lima (2006) in studies involving areas with similar environmental problems. The collection of core 1 took place directly in the river channel. The core 2.1 was also collected directly from the river channel, while core 2.2 was collected on the bank, about 1 meter away from the river channel. The collection of two cores downstream of the refinery is due to an apparent difference in the grain size of

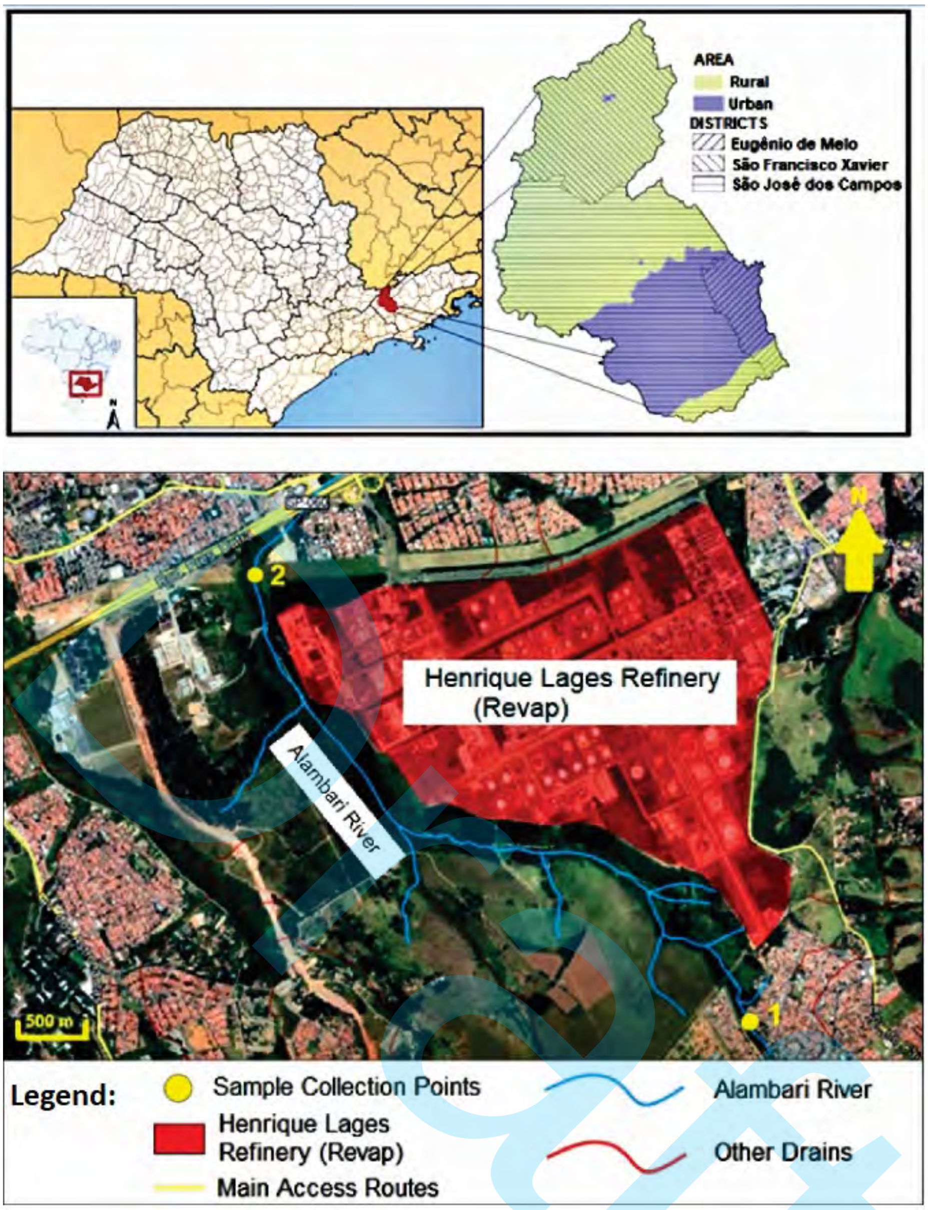

Figure 1: Location of (top) São José dos Campos city in São Paulo State, Brazil, and (bottom) Revap, drainages, access roads and two collection points of three sediment cores samples (1 at point 1, and 2.1, 2.2 at point 2).

the material as observed in the field work, with core 2.1 appearing to be of coarser grain size in relation to core 2.2.

The device utilized for the sediment core sampling consisted of a 5-cm diameter by 50-cm height PVC tube possessing inside another movable tube of smaller diameter. The equipment fully opened is 97-cm high, with a rubber existing between the tubes for helping in the suction, as well as two sites between them in order to hold the apparatus and to perform the sample suction due to the creation of a partial vacuum responsible by a pressure differential.

METHODS

The loss on ignition (LOI) method was used as a rough estimate of the percentage of total organic matter (OM) in the sediments. This is because the LOI data often express the OM + adsorbed water + water in crystal lattices and fluid inclusions + CO_2 of carbonates + SO_2 of sulfides (Faure, 1998). For evaluating this parameter, the samples were added to crucibles and weighed (1 g) on an analytical balance. The crucibles were taken to the muffle for firing at 500°C for two hours with subsequent natural cooling. Subsequently, a new weighing was carried out and the percentage of OM emanated during the firing was calculated.

For the grain size analysis, the layers of the sediment cores were properly prepared and later sieved in sieves of different meshes and, then, they were differentiated into very coarse sand (2.0-1.0 mm), coarse sand (1.0-0.5 mm), medium sand (0.5-0.25 mm), fine/very fine sand (0.25-0.063 mm), silt (0.063-0.031 mm) and silt together with clay (<0.031 mm). The moisture (MST) was evaluated from the total weight (TW) and dry weight (DW) of the sediment aliquots, according to the formula MST = [(TW-DW)/TW] × (100%). The porosity (ϕ) of the sediments was calculated by the following expression as reported by Argollo (2001): ϕ = (TW–DW) / TW + [DW (ρ_1/ρ_2 - 1)], where ρ_1 = water density (1 g/cm^3) and ρ_2 = sediment density (2.65 g/cm^3).

The chemical analysis of the sediments was realized by X-ray fluorescence (XRF). Discs of 4 cm in diameter were made for each of the 23 sediment aliquots as previously cut in segments of 5 cm in thickness by 5 cm in diameter. The choice of 5 cm rather than 1-2 cm thick slices was motivated by successful results obtained in previous investigations already realized for the same purpose (for instance, Bonotto & Lima, 2006; Sabaris, 2010; Matamet, 2013; Bonotto & García-Tenorio, 2014), and to avoid higher analytical costs and laboratorial time for processing larger number of segments related to each sediment core as well. The samples were prepared by the pressed powder method and were properly identified and packaged. The XRF allowed characterizing the main constituents throughout the sediment cores and possible minor ones that could indicate the presence of potential contaminants mostly coming from the urban environment or from Revap.

The quantification of the total ^{210}Pb (^{210}Pb$_t$) present in the samples was performed indirectly through alpha spectrometry of ^{210}Po, the "grandson" of ^{210}Pb, which is a product of the radioactive decay in the ^{238}U series (Ivanovich & Harmon, 1992). Such technique has been widely used to identify and quantify the alpha particles emitting radionuclides present in the natural decay series of ^{238}U, ^{235}U and ^{232}Th as reported in studies of environmental samples (García-Orellana & García-Léon, 2002; Loppi et al., 2003; Bonotto et al., 2005; Bonotto & Lima, 2006; Nery, 2009; Sabaris, 2010; Matamet, 2013; Bonotto & García-Tenorio, 2014; Nery & Bonotto, 2022).

The principle of isotopic dilution allowed determining the ^{210}Po activity as a function of the amount of the ^{209}Po tracer added. According to this principle, it occurs the mixture of a known number of added ^{209}Po atoms (activity = A_{209}) with an unknown number of ^{210}Po atoms (activity = A_{210}). After the complete isotopes homogenization, the results between the N_{210} and N_{209} scores obtained, respectively, in the ^{210}Po and ^{209}Po peaks present in the alpha spectrum allow determining the A_{210} value through the following equation:

$$\frac{A_{210}}{A_{209}} = \frac{N_{210}}{N_{209}} \tag{1}$$

In other words,

$$A_{210} = \left(\frac{N_{210}}{N_{209}}\right)_{measured} . A_{209} \tag{2}$$

In this study, the value of A_{209} added to each sample corresponded to 8 dpm, allowing determining chemical yields between 10% and 23%.

The "in-situ produced" ("supported") ^{210}Pb (^{210}Pb$_s$) was determined by gamma spectrometry with a NaI(Tl) scintillation detector based on the descriptions of Lima (2000). For calibration of the gamma spectrometer in uranium concentration, the same standards described by Casagrande and Bonotto (2018) were used, which exhibit known concentration of this radioelement. The readings of the eU (equivalent uranium = ^{226}Ra) were done considering the ^{214}Bi photopeak (1.76 MeV energy) and adopting the following calibration curve:

$$\log (eU) = 1.057 \times \log I_U + 2.578 \tag{3}$$

where, I_U is the effective intensity (counting rate per weight). ^{210}Pb$_s$ was calculated from the equation ^{210}Pb$_s$ = 0.16×eU, which takes into account the expected Rn atom fraction formed in the solid phase that will contribute to the ^{210}Pb$_s$ generation (Bonotto & Lima, 2006; Bonotto & García-Tenorio, 2014; Nery & Bonotto, 2022).

The analytical technique for the quantification of total ^{210}Pb consisted of the digestion of sediments through chemical processes so that ^{210}Po can be extracted and deposited on a copper disc to, afterwards, quantify it by means of alpha spectrometry. The radioactive equilibrium condition allows determining the total ^{210}Pb values in the samples using the measured values for ^{210}Po (Ivanovich & Harmon, 1992).

The alpha spectrometry is based on the detection of the energy of alpha particles (2 protons and 2 neutrons; charge 2+), whose relatively large mass rapidly interacts with a Si detector of the surface barrier type (Knoll, 1989). This allows obtaining the spectra, enabling the radionuclides identification and determination of the activity concentration in the sample. The measurements in the alpha spectrometer are carried out in a vacuum to prevent the alpha particles from being absorbed by the air. The deposited sample must contain a very thin, compact and uniform layer to avoid certain self-absorption problems and, thus, improve the resolution of the spectra (Ivanovich & Harmon, 1992).

The excess ^{210}Pb (^{210}Pb$_{exc}$) was determined by the difference between total ^{210}Pb and "in-situ produced" ^{210}Pb. The obtained ^{210}Pb$_{exc}$ data were input values for the CRS model, satisfying the following equation (Krishnaswami et al., 1971; Appleby & Oldfield, 1978; El-Daoushy, 1988; Kotarba et al., 2002):

$$A_x = A_0 . e^{-\lambda . t} \quad \text{or} \quad t = (1/\lambda) . ln\, (A_0/A_x) \tag{4}$$

where, t is the age; λ is the ^{210}Pb decay constant (0.0311 yr^{-1}); and A_0 and A_x (in dpm/g) are, respectively, the total ^{210}Pb$_{exc}$ inventory and ^{210}Pb$_{exc}$ inventory from the layer at depth x to the bottom of the sediment core. The following formula was also adopted in the calculation (Kotarba et al., 2002):

$$r_n = (h_n - h_{n-1}) / (t_n - t_{n-1}) \tag{5}$$

where, r_n is the sedimentation rate for the interval between centers of the $n-1$ and n-*th* layer; and h_n and t_n are the mass depth and age of the n-*th* layer, $h_0 = 0$, $t_0 = 0$.

RESULTS AND DISCUSSION

Grain Size and LOI Analysis

Table 1 reports the results of the grain size analysis of the sediment cores in this study, showing that the predominant size in the cores is sand. A greater quantity of sand-sized sediments occurs in cores 1 and 2.1 taken directly from the Alambari River channel. The core 2.2 was taken from the banks of the same river, presenting smaller amounts of sand and greater percentage of silt and clay in relation to cores 1 and 2.1. Such site presents a sediment deposition dynamics different from the sedimentation dynamics along the river channel. Thus, on the banks of the river, finer sediments tend to be deposited when the river overflows and carries them, mostly in suspension, to the banks of the flood. This justifies the more accentuated presence of finer sediments (silt + clays) found in core 2.2.

In core 1, the average percentage of sand from the different sections is 93.61%, while silt and clay represent 6.39% of the sediments. In core 2.1, the average percentage of sand from the different sections is 96.88%, while silt and clay represent 3.12% of the sediments. In core 2.2, the average percentage of sand from the different sections is 81.46%, while silt and clay represent 18.54% of the sediments. River waters, during flood periods, distribute weathering materials from the crystalline basement to their overflow plains, despite the reduced energy gradient. This transport mechanism has already been described by Fúlfaro et al. (1979) to explain the high percentage of clay on the margins of drainages. The moisture and porosity are higher in core 2.2 relatively to cores 1 and 2.1 (Table 1).

Table 1 also reports the LOI data obtained in this study (mean value between 0.9 and 8.2%). Matamet (2013) found out that there is a direct relationship between LOI and OM, justified by the amount of water present in the organic matter. The mean LOI (OM) value is different for each core (Table 1), i.e., in cores 1 and 2.1, taken from the river channel; a smaller amount of LOI can be observed relatively to core 2.2, taken from the banks of the river. The maximum and minimum LOI values are, respectively, 1.7 and 0.2% in core 1, 3.5 and 0.6% in core 2.1, and 10.5 and 5% in core 2.2 (Table 1).

There is also a significant correlation between finer-grained sediments and LOI. In this way, OM is directly associated with finer sediments and greater amounts of metals. Thus, OM is available in places that contain more nutrients to grow, being mainly associated with the core having less silica (SiO_2) and higher concentration of iron, aluminum and other constituents.

The correlations between depth, LOI, and the percentage of finer-grained sediments (bottom sediments = silt + clay) are shown in Figure 2. The LOI values and bottom sediments (silt + clay) in core 2.1 show a significant correlation. In the graphs of the three cores (Figure 2), the trend lines are variable for each sample. In core 1, the Pearson correlation coefficient (r) is 0.578 and 0.398 for LOI and bottom sediments, respectively; and in core 2.1, r is 0.945 and 0.829 for LOI and bottom sediments, respectively. In core 2.2, r is -0.406 and -0.488 for LOI and bottom sediments, respectively. Such data demonstrate, for core 2.1, the direct correlation between LOI and the finer-grained sediments. According to the trend lines of the graphs, Figure 2 suggests in cores 1 and 2.1 a tendency of increasing the percentages of LOI and finer-grained sediments as the profile depth increases. In core 2.2, there is an inverse correlation, with a tendency to decrease the percentages of LOI and finer-grained sediments as the profile depth increases.

Chemical Composition of the Sediments

Table 2 summarizes the statistics of mean, median, standard deviation, maximum and minimum values of the oxides determined in the analysis by X-ray fluorescence spectrometry of sediments from cores 1, 2.1, and 2.2.

In the three cores, silica (SiO_2) is the main constituent in the sediments (average concentration ranging between 41.63% and 82.58%). A greater amount of SiO_2 was found in samples 1 and 2.1, which were taken from the Alambari River channel. In sample 2.2, taken from the banks of the river channel, the average silica concentration was the lowest (41.63%). Sample 1, taken upstream of the Alambari River channel, showed a lower SiO_2 concentration (73.13%) compared to sample 2.1 (82.58%), taken downstream of the Alambari River channel. The greater amount of leached silica downstream of the basin indicates the high mobility of this constituent in relation to possible source areas, since the sediment source areas are closer to the place where sample 1 was taken.

Following silica, aluminum (Al_2O_3; mean concentration = 8.79-27.16%) and iron (Fe_2O_3; mean concentration = 5.2-25.38%) also exhibit high concentrations, as well as potassium (K_2O; mean concentration = 1.16-1.46%) and titanium (TiO_2; mean concentration = 0.49-1.92%) which average concentration exceeds 1% in practically all cores. Aluminum, iron, potassium and titanium showed higher concentrations in core 1 compared to core 2.1.

Table 3 presents the range of the Pearson correlation coefficient (r) among SiO_2, the different oxides and LOI for the cores 1, 2.1, and 2.2. The weak, moderate and strong correlations are based on the r values also reported in Table 3. According to this criterion, it occurs several strong correlations (positive or negative) of SiO_2 with most oxides (Table 3).

One relevant finding of this study is the inverse relationship between silica and LOI in the three sampling sites (Table 3) (r = -0.958 in core 1; r = -0.934 in core 2.1; r = -0.836 in core 2.2), indicating a trend in the Alambari River basin that the silica values are higher when the LOI values decrease. Beyond modifying the bulk density and porosity of soils and sediments, the OM also influences their specific surface (area per mass, often expressed in m^2/g),

Table 1: Results of grain size analysis, LOI, moisture and porosity of the sediment cores collected in Alambari River, São José dos Campos, São Paulo State, Brazil.

Depth (cm)	Very coarse sand (%)	Coarse sand (%)	Medium sand (%)	Fine sand (%)	Silt + clay (%)	LOI (%)	Moisture (%)	Porosity (%)
Core 1								
0-5	2.54	11.3	45.76	39.66	0.64	0.3	25.3	47.3
5-10	1.36	6.69	57.82	32.73	1.04	0.2	22.1	43.0
10-15	0.51	4.56	41.65	51.01	1.74	0.5	23.0	44.2
15-20	0.22	0.94	8.37	83.14	7.02	0.7	27.2	49.8
20-25	4.62	9.64	40.41	28.41	16.90	1.6	34.6	58.3
25-30	7.76	8.76	40.87	34.68	7.93	1.7	24.9	46.8
30-35	2.79	7.67	51.75	30.71	6.75	0.7	22.8	43.8
35-40	4.08	19.18	42.72	26.15	7.36	0.9	20.6	40.8
40-45	3.90	18.79	48.15	20.35	8.19	1.1	21.2	41.6
Mean	3.08	9.72	41.94	38.53	6.39	0.9	24.6	46.2
Core 2.1								
0-5	0.41	19.88	69.56	8.91	0.87	0.6	41.6	65.3
5-10	0.78	17.19	69.73	10.45	1.72	1.1	36.2	60.1
10-15	1.87	22.33	63.97	10.05	1.42	1.9	31.1	54.5
15-20	1.48	23.87	60.88	11.50	1.94	1.5	23.9	45.4
20-25	2.18	21.04	59.78	12.58	3.99	1.9	24.7	46.4
25-30	7.20	27.62	48.92	11.51	4.47	2.8	23.1	44.3
30-35	3.37	32.37	45.37	11.47	7.43	3.5	20.5	40.6
Mean	2.47	23.47	59.74	10.92	3.12	1.9	28.7	51.0
Core 2.2								
0-5	1.50	15.41	34.65	26.35	22.09	10.5	63.5	82.2
5-10	1.36	15.82	35.05	23.18	24.55	8.1	57.2	78.0
10-15	1.92	19.14	34.34	21.23	23.32	7.5	42.1	65.9
15-20	8.83	20.83	31.34	22.15	16.69	10.3	63.7	82.3
20-25	6.77	16.34	58.53	11.77	6.65	5.0	63.2	82.0
25-30	8.87	23.03	35.41	17.33	15.34	7.4	65.0	83.1
30-35	3.83	16.03	32.17	26.66	21.20	8.5	68.3	85.1
Mean	4.72	18.08	37.35	21.23	18.54	8.2	60.4	79.8

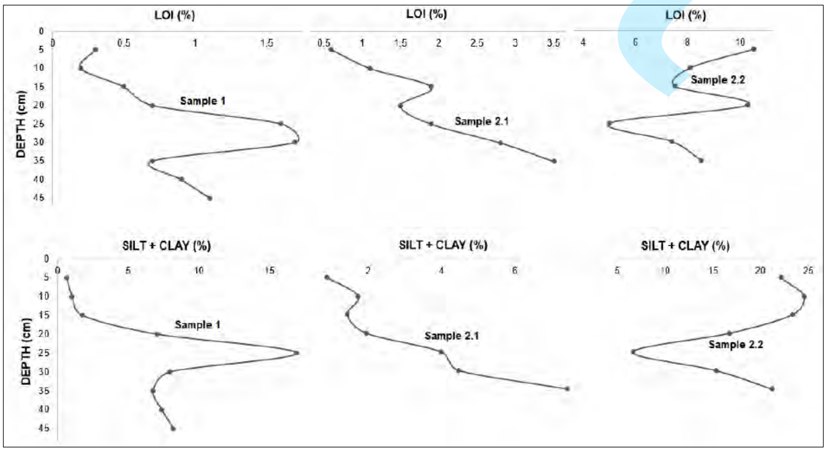

Figure 2: Graphs of the relationships among depth (in cm), LOI (in %) and bottom sediments (silt + clay, in %) in the sediment cores collected in Alambari River, São José dos Campos, São Paulo State, Brazil.

Table 2: Values (in %) of the main oxides analyzed in the sediment cores collected in Alambari River, São José dos Campos, São Paulo State, Brazil.

Depth (cm)	SiO_2	Al_2O_3	Fe_2O_3	K_2O	TiO_2	CaO	MgO	Na_2O	P_2O_5	SO_3	BaO	MnO
Core 1												
0-5	88.59	5.56	2.25	1.21	0.47	0.32	0.08	0.29	0.06	0.03	0.18	0.02
5-10	87.87	6.48	2.29	1.21	0.48	0.29	0.07	0.26	0.06	0.03	0.03	0.01
10-15	80.20	11.62	4.28	1.37	0.85	0.39	0.13	0.26	0.08	0.05	<0.01	0.02
15-20	69.81	18.77	7.10	1.55	1.29	0.49	0.14	0.18	0.12	0.06	0.02	0.03
20-25	56.32	27.02	10.97	1.49	1.96	0.68	0.25	0.13	0.23	0.24	0.03	0.06
25-30	58.01	24.95	11.32	1.70	1.68	0.53	0.30	0.14	0.18	0.14	0.27	0.22
30-35	73.47	16.45	5.91	1.56	1.02	0.42	0.21	0.27	0.11	0.07	<0.01	0.05
35-40	72.91	16.87	6.20	1.42	1.07	0.38	0.18	0.24	0.11	0.09	0.07	0.06
40-45	71.03	17.63	6.86	1.63	1.15	0.46	0.28	0.26	0.13	0.08	<0.01	0.07
Average	73.13	16.15	6.35	1.46	1.11	0.44	0.18	0.23	0.12	0.09	0.07	0.06
Median	72.91	16.87	6.20	1.49	1.07	0.42	0.18	0.26	0.11	0.07	0.03	0.05
Standard Deviation	11.36	7.34	3.25	0.17	0.50	0.12	0.08	0.06	0.06	0.07	0.09	0.06
Core 2.1												
0-5	90.72	3.20	3.05	1.22	0.13	0.18	<0.01	0.20	<0.01	0.04	0.04	0.03
5-10	89.27	3.85	3.93	1.09	0.15	0.20	0.04	0.20	0.04	0.05	0.20	0.05
10-15	88.32	4.53	4.08	1.17	0.19	0.23	0.04	0.24	0.05	0.08	0.06	0.06
15-20	87.20	5.79	3.59	1.06	0.29	0.56	0.04	0.19	0.03	0.07	0.20	0.09
20-25	84.82	7.52	4.41	1.06	0.40	0.20	0.05	0.18	0.05	0.12	0.18	0.10
25-30	74.94	14.06	7.30	1.10	0.82	0.23	0.13	0.18	0.08	0.21	0.21	0.13
30-35	62.83	22.60	10.08	1.41	1.44	0.21	0.18	0.12	0.11	0.37	0.07	0.13
Average	82.58	8.79	5.20	1.16	0.49	0.26	0.07	0.19	0.05	0.13	0.14	0.08
Median	87.20	5.79	4.08	1.10	0.29	0.21	0.04	0.19	0.05	0.08	0.18	0.09
Standard Deviation	10.16	7.10	2.55	0.12	0.48	0.13	0.06	0.04	0.04	0.12	0.08	0.04
Core 2.2												
0-5	36.43	27.68	30.64	1.10	1.90	0.32	0.27	<0.01	0.18	0.42	0.25	0.36
5-10	37.60	28.66	28.70	1.16	2.01	0.31	0.25	<0.01	0.17	0.35	0.11	0.24
10-15	40.48	30.52	23.54	1.32	2.20	0.29	0.27	<0.01	0.16	0.43	0.11	0.17
15-20	35.49	28.24	26.84	1.28	2.03	0.32	0.26	0.05	0.16	0.46	<0.10	0.38
20-25	64.20	18.55	12.83	1.47	1.16	0.29	0.18	0.12	0.13	0.27	<0.10	0.35
25-30	39.30	28.04	27.15	1.23	2.04	0.31	0.25	0.03	0.15	0.29	0.10	0.61
30-35	37.93	28.43	28.00	1.14	2.07	0.37	0.25	0.03	0.18	0.35	0.12	0.72
Average	41.63	27.16	25.38	1.24	1.92	0.32	0.25	0.03	0.16	0.37	0.10	0.40
Median	37.93	28.24	27.15	1.23	2.03	0.31	0.25	0.03	0.16	0.35	0.11	0.36
Standard Deviation	10.09	3.90	5.94	0.13	0.34	0.03	0.03	0.04	0.02	0.07	0.08	0.20

Table 3: Correlation of silica (SiO_2) with other oxides and LOI. Direct (+) or inverse (-) correlations are indicated and the range of the Pearson's correlation coefficient (r) as well.

Pearson's r value	Core 1	Core 2.1	Core 2.2
Strong correlation $\|0.6\| < r < \|1\|$	(-)Al_2O_3, (-)Fe_2O_3, (-) K_2O, (-)TiO_2, (-)CaO, (-)MgO, (+)Na_2O, (-)P_2O_5, (-)SO_3, (+)CoO, (-)MnO, (-)LOI	(-)Al_2O_3, (-)Fe_2O_3, (-)K_2O, (-)TiO_2, (-)MgO, (+)Na_2O, (-)P_2O_5, (-)SO_3, (+)CoO, (-)MnO, (-)LOI	(-)Al_2O_3, (-)Fe_2O_3, (+)K_2O, (-)TiO_2, (-)MgO, (+)Na_2O, (-)P_2O_5, (-)SO_3, (+)CoO, (-)LOI
Moderate correlation $\|0.3\| < r < \|0.6\|$	none	none	(-)CaO, (-)BaO
Weak correlation $0 < r < \|0.3\|$	(-)BaO	(+)CaO, (+)BaO	(-)MnO

since 1% of OM in porous matrices may cause an increase of the specific surface area of about 7 m^2 (Kiehl, 1977). Consequently, other parameters are also significantly affected like the cation exchange capacity, cation adsorption, and percentage of water retention in soils/sediments, which, in general, increases during rising of the specific surface area. Therefore, the SiO_2-LOI relationships in this study suggest that the decrease in SiO_2 concentration should be accompanied by an increase in the specific surface area of the sediments due to the LOI (OM) enhancement, implying an enhanced cation exchange/adsorption capacity. Such behavior has been already pointed out in other hydrographic basins in Brazil (see, for instance, Bonotto & Lima, 2006; Nery, 2009; Sabaris, 2010; Bonotto & García-Tenorio, 2014). In this study, SiO_2 showed inverse relationship in practically all cores with Al_2O_3, Fe_2O_3, TiO_2, K_2O, CaO, MgO, P_2O_5, and MnO (Table 3), while the OM role on the adsorption of several oxides and formation of metal-organic compounds is chiefly evidenced by the direct significant correlations among LOI and Al_2O_3, Fe_2O_3, TiO_2, MnO, and P_2O_5. Multivariate analysis (multiple regression) also confirmed the OM role on the adsorption of several oxides analyzed and their inverse relationships with silica in the core sediments as outlined by the equations reported in Table 4.

Sedimentation Rates and Chronological Implications

In the present work, the CRS (Constant Rate of ^{210}Pb Supply) mathematical model was used for obtaining sedimentation rates. According to the assumptions of the CRS model, variable sedimentation rates occur along the sediment profile. The great advantage of the CRS model is the possibility of calculating the age of sediments as well as variations in the sedimentation rate in an aquatic environment.

As described in the Methods section, the quantification of ^{210}Pb in the samples was performed indirectly by alpha spectrometry of ^{210}Po. The *in-situ* produced ^{210}Pb was obtained from the uranium equivalent (eU = ^{226}Ra) and application of a correction factor due to the ^{222}Rn escape, which corresponds to 0.16 (Lima, 2000). Such factor arises from the ^{222}Rn loss estimation during laboratory timescale experiments reported by Bonotto and Caprioglio (2002) for different samples of sedimentary rocks crushed to grain sizes compatible with the sediment cores in this study. Those assays yielded an average value of 0.84 for the ^{222}Rn emanation coefficient (E) from the rock matrices and soils/sediments, which allowed estimating that only 16% of the ^{222}Rn generated by ^{226}Ra decay contribute to the production of ^{210}Pb.

To determine the sedimentation rate, the ^{210}Pb method needs precise values of the excess ^{210}Pb along the sediment column, which are obtained from the values of ^{210}Pb (total) and ^{210}Pb (*in-situ* produced) (Lima, 2000). The excess ^{210}Pb activity was calculated from the difference between the total ^{210}Pb activity and *in-situ* produced ^{210}Pb activity as reported in Table 5. The excess ^{210}Pb activity does not systematically decrease according to the depth increase, in which case it would be possible to adopt the CF:CS model for estimating the sedimentation rates (Bonotto & García-Tenorio, 2014). Therefore, it is justifiable the choice of the CRS model for such purpose as it takes into account processes that may influence the distribution and deposition of the available ^{210}Pb in the sediment column, both vertically and horizontally (Bonotto & García-Tenorio, 2014). Table 6 presents the relevant data for using the CRS model to determine the deposition time, deposition year, and sedimentation rates by ^{210}Pb.

To calculate the age of the cores, the activity value (in dpm) of the excess ^{210}Pb was initially used. The cumulative activity divided by the sum of the activities yields a value, whose natural logarithm generates a new result. This last value must be multiplied by 32.154, which is the reciprocal of the ^{210}Pb disintegration constant, generating the layer age. From the data reported in Table 6, it can be highlighted that the oldest sediment layer is found in core 1 (upstream of Revap), which was deposited about 74 years ago (~1946). In core 2.1, the oldest sediments were deposited 34 years ago (~1986),

Table 4: Regression equations obtained by multivariate analysis taking into account the concentrations of LOI and major oxides in the three sediment cores analyzed in this study.

Regression equation	
Core 1	
$SiO_2 = 98.78 - 1.03Al_2O_3 - 0.39Fe_2O_3 - 0.28K_2O - 2.22TiO_2 - 4.96CaO + 0.53MgO - 6.71P_2O_5 - 12.37MnO$	$(r^2=1)$
$LOI = 4.08 - 0.075Al_2O_3 + 1.42Fe_2O_3 - 3.71K_2O - 4.88TiO_2 + 2.93CaO + 7.26MgO - 17.48P_2O_5 - 12.10MnO$	$(r^2=1)$
Core 2.1	
$SiO_2 = 97.48 - 1.09Al_2O_3 - 0.30Fe_2O_3 - 1.69K_2O - 0.0001TiO_2 - 21.31MgO - 0.0001P_2O_5 - 2.58MnO$	$(r^2=1)$
$LOI = 4.82 + 6.38Al_2O_3 - 4.69Fe_2O_3 - 72.22TiO_2 + 36.08MgO + 73.47P_2O_5 - 68.24MnO$	$(r^2=1)$
Core 2.2	
$SiO_2 = 90.36 + 1.35Al_2O_3 - 1.01Fe_2O_3 - 20.99TiO_2 - 94.17MgO + 23.24P_2O_5$	$(r^2=0.98)$
$LOI = -1.99 - 1.34Al_2O_3 + 0.13Fe_2O_3 + 6.99TiO_2 + 105.10MgO + 24.82P_2O_5$	$(r^2=0.88)$

Table 6: Determination of the deposition time, deposition year, and sedimentation rates of each section of the three cores.

Depth (cm)	Mass depth (g/cm^2)	$^{210}Pb_{exc}$ (dpm/g)[1]	ln (Cumulated activity/ Total activity)	Deposition time (years)	Deposition Year	Sedimentation rate ($g/cm^2.yr$)
Core 1						
Top-5	0.925	nc	nc	nc	nc	nc
5-10	5.919	0.519	0	0	2020	nc
10-15	5.796	0.527	0.062	2.012	2018	2.880
15-20	6.004	0.622	0.130	4.189	2016	2.757
20-25	5.008	2.410	0.216	6.966	2013	1.803
25-30	5.970	1.475	0.646	20.782	1999	0.432
30-35	6.112	1.284	1.044	33.597	1987	0.476
35-40	6.177	0.881	1.600	51.451	1969	0.345
40-45	6.491	0.848	2.312	74.363	1946	0.283
					Mean	1.282
Core 2.1						
Top-5	3.473	nc	nc	nc	nc	nc
5-10	4.481	0.530	0	0	2020	nc
10-15	4.817	0.352	0.069	2.245	2018	2.145
15-20	5.665	0.527	0.119	3.830	2016	3.572
20-25	5.332	1.813	0.197	6.359	2014	2.108
25-30	4.419	1.931	0.527	16.968	2003	0.416
30-35	2.747	2.707	1.066	34.283	1986	0.158
					Mean	1.680
Core 2.2						
Top-5	1.049	4.644	0	0	2020	nc
5-10	1.403	6.290	0.086	2.792	2017	0.502
10-15	1.650	10.036	0.217	7.007	2013	0.391
15-20	1.936	8.692	0.470	15.140	2005	0.238
20-25	3.693	4.064	0.757	24.360	1996	0.400
25-30	2.643	7.570	0.926	29.785	1990	0.487
30-35	2.136	14.543	1.345	43.260	1977	0.158
					Mean	0.363

[1] excess ^{210}Pb ($^{210}Pb_t$ - $^{210}Pb_s$); nc = not calculated

while the oldest sediments were deposited 43 years ago (~1977) in core 2.2.

To determine the sedimentation rate from the CRS model, data on dry mass/area (g/cm²) and deposition time of each layer must be available. The dry mass varies in each section of the core. The area of the sections is constant (19.635cm²) as all cores are 5 cm in diameter. The division of the dry mass by the deposition time of the sediment layer allows estimating a variable sedimentation rate associated with the strata deposition in the sedimentary column. Table 6 shows the different sedimentation rates found for the three sediment cores.

As already mentioned, the CRS model generates variable sedimentation rates along the sediment profile. The sedimentation rate determined by this model allows identifying any inconsistency in the sediment deposition due to the different contribution of the sediment depot or other variables over time, which were responsible for the increase or decrease in the sedimentation rates. The CRS model is often more suitable for dating environments very influenced by anthropic activities, as this method considers the changes suffered by them over the time period.

In core 1, taken from the river channel, the sedimentation rate of the sections varies from 0.283 to 2.88 g/cm².year (mean = 1.282 g/cm².year), corresponding to a linear sedimentation rate of 0.60 cm/year. The sedimentation rate showed a gradual growth from the oldest sediment sections to the most recent ones.

In core 2.1, also taken from the river channel, the sedimentation rate varies from 0.158 to 3.572 g/cm².year (mean = 1.68 g/cm².year), corresponding to a linear sedimentation rate of 1.02 cm/year. The sedimentation rate tended to increase from the older sediment sections to the more recent ones, similarly to core 1.

In core 2.2, taken from the banks of the river channel, the sedimentation rate varies from 0.158 to 0.502 g/cm².year (mean = 0.363 g/cm².year), corresponding to a linear sedimentation rate of 0.81 cm/year.

In general, in the three cores, the most recent sections have a higher sedimentation rate than the oldest ones. In samples 1 and 2.1, the sedimentation rates tend to exhibit a more pronounced increase towards the most recent sections, compared to sample 2.2. It can be verified direct correlations between the deposition time and depth (Figure 3) and inverse correlations between the sedimentation rate and depth for cores 1 and 2.1 (Figure 4). Thus, the trend lines in Figure 3 indicate that the deposition time tends to increase according to the depth increase. The values of Pearson's correlation coefficients for these straight lines are r = 0.953, r = 0.895 and r = 0.798 for cores 1, 2.1 and 2.2, respectively; and these coefficients are r = -0.917 and r = -0.802 for cores 1 and 2.1, respectively, considering the plots of the sedimentation rate *vs.* depth (Figure 4). These graphs suggest that the sedimentation rate tends to decrease as depth increases for cores 1 and 2.1 and, therefore, such rates are inversely correlated with the deposition time.

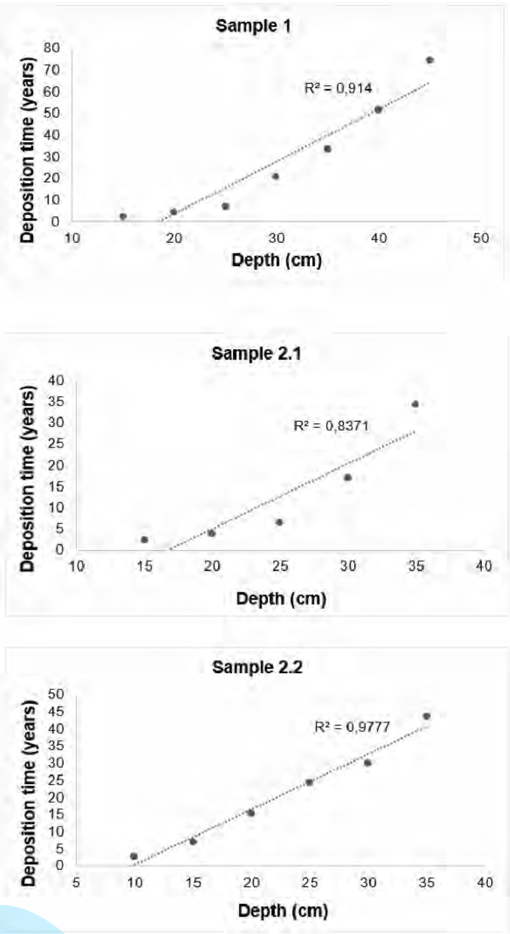

Figure 3: Relationship of the deposition time (in years) *vs.* depth (in cm) in the sediment cores 1, 2.1, 2.2 collected in Alambari River, São José dos Campos, São Paulo State, Brazil.

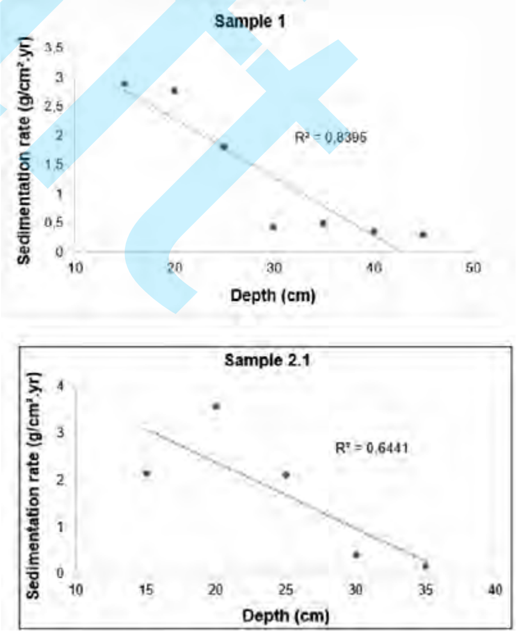

Figure 4: Relationship of the sedimentation rate (g/cm².year) *vs.* depth (in cm) in the sediment cores 1 and 2.1 collected in Alambari River, São José dos Campos, São Paulo State, Brazil.

Trace Constituents as Potential Pollutants

Recurrently, oil spill accidents originating from Revap have reached the Alambari River. The pipeline system that directs rainwater and oils from the refinery failed several times with overflows and leaks, which culminated in pipelines that flow into the Alambari River transporting Revap oils to the river, harming the local ecosystem and contaminating the waters and sediments of the drainage.

The constituents identified in smaller amounts (trace elements) by means of XRF spectrometry may indicate eventual anthropic influences (PAI = possible anthropogenic input) on the Alambari River basin. In addition to the oxides reported in Table 2, other constituents can be highlighted whose origin may be related to the Revap activities, among them, palladium (Pd), nickel (Ni) and vanadium (V).

Palladium has been used as a heterogeneous catalyst for reactions in the distillation of petroleum components, because it is a great hydrogen adsorber. Pd was measured at or above the detection limit (DL = 0.01%) in the sediments downstream of the refinery (cores 2.1 and 2.2). Upstream of Revap, in core 1, Pd was always below DL. In core 2.1, Pd was at or above the DL in 3 sections (Figure 5): 5-10 cm (0.02%; year 2020); 10-15 cm (0.01%; year 2018); 30-35 cm (0.01%; year 1986). In core 2.2, Pd is at the DL between 25 and 30 cm depth, with the deposition year corresponding to 1990 (Figure 5). The Pd level of cores 2.1 and 2.2 is equal (0.01%), practically corresponding to the same deposition year, respectively, 1986 and 1990. Palladium itself is not a highly toxic element, but it is a trace constituent of important use in the petroleum industry for the catalysis of distillate petroleum fractions. Thus, the Pd levels at or above the DL in the sediment sections shown in Figure 5 could indicate some contamination of the Alambari River by the oils coming from Revap, which would carry out the Pd deposited into the sediments downstream of the refinery. However, there is a lack of data of regional baseline geochemical Pd levels for comparison purposes in the study area and, currently, such hypothesis should be disregarded.

Beyond the different atoms of carbon or hydrogen in an organic compound (heteroatom), in petroleum, V and Ni stand out for being the most abundant metals. Kenny (2013) reported V and Ni levels of 0.05-298.5 ppm and 0.54-193.8 ppm, respectively, for crude oils from fields in different nations, meaning that these metals are present in quite variable concentration in oils from around the world. In Brazil, Barela (2014) measured V and Ni concentration of 10.2-25.7 ppm and 9.8-16.1 ppm, respectively, in three samples of petroleum provided by Petrobras. Therefore, these data indicate that V and Ni can be found in significant amount in petroleum products. The presence of compounds of these metals in petroleum matrices has been considered important to trace the geological origin of crude oil, as well as migration and maturation, in addition to having interference in fractionation, corrosion and environmental pollution processes (Barela, 2014; Lorenzoni, 2019). The ratio between Ni and V can also be used as an indicator of the origin of oil, allowing differentiating between continental and maritime (Kenny, 2013).

Nickel is a metallic element and it is not a very toxic metal. Vanadium is an essential mineral constituent for the functioning of our body. However, it causes intoxication when its concentration greatly increases in the body. Excess vanadium can be toxic, with symptoms depending on the chemical form and mode of contamination. In this study, it was possible to identify the presence of Ni (as NiO) and V (as V_2O_5) at or above the DL in sample 2.2 (Figure 5). Nickel was at the DL of 0.01% from the top of the profile up to 15 cm depth (years 2020, 2017 and 2013), reaching 0.02% at 15-20 cm depth (year 2005). In this profile (2.2), vanadium at or above DL was characterized in 3 sections: from the top to 5 cm depth (0.02%; year 2020), from 10 to 15 cm depth (0.01%; year 2013) and from 15 to 20 cm depth (0.02%; year 2005) (Figure 5). The greater amount of Ni and V in the sections of sample 2.2 could indicate an influence of the oil derivatives from the adjacent refinery.

In order to check this hypothesis, available geochemical data of sediments from Tremembé Formation in Taubaté Basin (Sallun & Diniz, 2016) can be used as regional baseline values for comparison purposes in the study area. Sallun and Diniz (2016) reported V and Ni levels of 35-162 ppm (mean = 112 ppm) and 10-56 ppm (mean = 33 ppm), respectively, when it was analyzed 39 samples of a sediment profile obtained of a drill core from a deep tubular well. The average V concentration at or above the DL in the sediment sections shown in Figure 5 corresponds to 95.2 ppm, which is practically equivalent to the mean V baseline geochemical level of 112 ppm, as reported by Sallun and Diniz (2016). Thus, there is no indication that the V found downstream of the refinery could denote its input as contaminant from petroleum derivatives coming from Revap.

The average Ni concentration at or above the DL in the sediment sections shown in Figure 5 corresponds to 94.3 ppm that is almost three times higher than the mean Ni baseline geochemical level of 33 ppm (Sallun & Diniz, 2016). Therefore, this trace metal could be a useful fingerprint to track eventual sediment contamination coming from Revap due to petroleum derivatives. However, the presence of Ni in the sediments may be associated with other anthropic activities because it is also used in the process of melting metal alloys, as a catalyst, and in pesticides. São José dos Campos is a scientific and technological pole with important companies and relevant teaching and research centers. Additionally, it is a military and metallurgical material technopole, hosting the largest aerospace complex in Latin America, with big industries such as Embraer

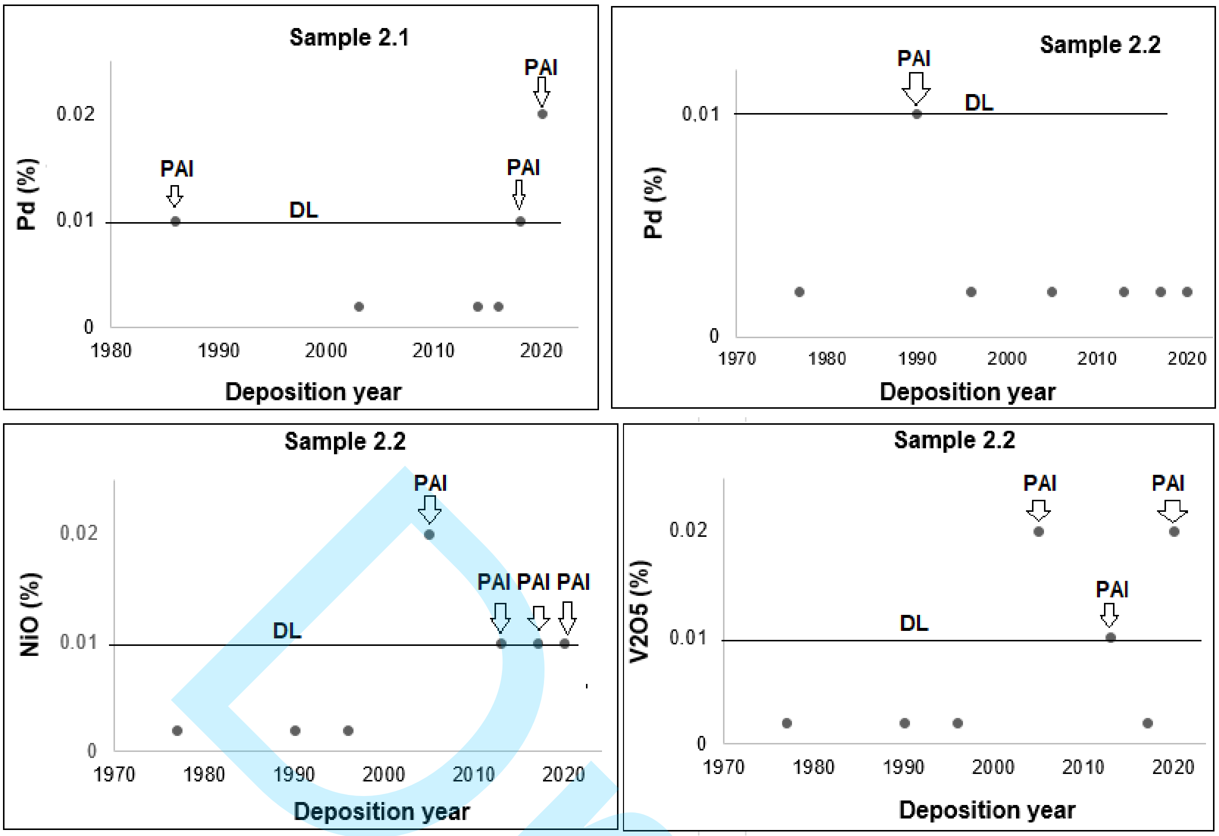

Figure 5: Plots of the Pd, NiO and V_2O_5 concentration against the deposition year for the sediment profiles 2.1 and 2.2. DL = detection limit. PAI = possible anthropogenic input.

(Brazilian aeronautical company). Alambari River is a watercourse that crosses the urban area of the municipality and, consequently, there are several potential sources for the Ni contamination in the sediments in addition to the petroleum derivatives such as the use of alloys in the manufacturing of aircrafts, ships, military vehicles, spacecrafts and missiles.

Thus, the Pd, Ni and V levels found downstream of Revap could indicate their inputs as contaminants from petroleum derivatives coming from the refinery. However, the lack (for Pd) and availability (for V) of regional baseline geochemical values, as well as the industrial activities developed in São José dos Campos, do not unequivocally permit to point out the dominant source responsible for the sediment contamination. Future researches are envisaged to focus these and other trace elements, adopting more sensitive analytical techniques like the inductively coupled mass spectrometry (ICP-MS) in order to get an improved scenario of these initial findings.

CONCLUSIONS

The data obtained in this study were analyzed and correlated with each other, providing inferences from several relationships found in the cores, including possible contaminants coming from the Henrique Lage Refinery (Revap). The grain size analysis of the sediments allowed concluding that the increase in the amount of silt and clay-sized sediments is directly proportional to the increase of the loss on ignition (LOI). Silica (SiO_2) is the main constituent in all three cores analyzed, with average concentrations ranging between 41.63% and 82.58%. The greater amount of leached silica downstream of the basin indicates the high mobility of this constituent in relation to possible source areas, since the sediment source areas are closer to the place where core 1 was taken from. Aluminum (Al_2O_3), iron (Fe_2O_3), potassium (K_2O) and titanium (TiO_2) are oxides considered to have low mobility along the drainage system, when comparing samples taken along the river channel. Inverse significant correlations were obtained between SiO_2 and these oxides, as well as direct relationships between LOI and them, confirming the results of previous investigations held in other Brazilian hydrographic basins. The oldest sediment is found at 45 cm depth in core 1, located upstream of Revap, which was deposited about 74 years ago (~1946). In cores 2.1 and 2.2 located downstream of the refinery, the oldest sediments were deposited 34 years ago (~1986) and 43 years ago (~1977), respectively. The sedimentation rate range is 0.283-2.88 g/cm².year for core 1; 0.159-3.573 g/cm².year for core 2.1; and 0.159-0.502 g/cm².year for core 2.2. Each respective linear sedimentation rate corresponded to 0.60, 1.02, and 0.81 cm/year. An inverse correlation was identified between the deposition time of the sediment layer and the sedimentation rate, while the depth is directly related to the deposition time. The X-ray fluorescence spectrometry allowed identifying concentrations of palladium, nickel and vanadium at or above the detection limit (DL), which could indicate an eventual influence of the Revap activities in the Alambari River basin. Palladium (Pd) is of important use in the petroleum industry in the catalysis of distillate petroleum fractions. Nickel (Ni) and vanadium (V) showed values at or above the DL in core 2.2, which was taken from the riverbanks. However, several other industrial activities developed in São José dos Campos may also be responsible for Ni inputs in the Alambari River watercourse. Additionally, for Pd, any regional baseline geochemical value is absent, whilst, for V, such parameter practically indicates similarity to the concentrations found in the sediments analyzed in this study. Therefore, in view of these findings, it is not possible unequivocally to point out the dominant source responsible for the release of these metals into the sediments, suggesting the need of further studies in order to achieve such purpose.

ACKNOWLEDGEMENTS

The authors are grateful to National Council for Scientific and Technological Development (CNPq), Brazil, for the scholarship to JPMM. Two anonymous reviewers are greatly thanked for helpful comments that improved the readability of this manuscript.

REFERENCES

Appleby, P. G., and F. Oldfield, 1978, The calculation of lead-210 dates assuming a constant rate of supply of unsupported ^{210}Pb to the sediment. Catena 5: 1–8. doi: 10.1016/S0341-8162(78)80002-2

Argollo, R. M., 2001. Chronology of the recent sedimentation and deposition of heavy metals at Baía de Todos os Santos using Pb-210 and Cs-137. PhD Thesis. Federal University of Bahia - UFBa. Salvador, BA, Brazil, 104 pp (in Portuguese).

Barela, P. S., 2014, Determination of nickel and vanadium in petroleum: study of different sample pretreatment methods. Monography. Federal University of Rio Grande do Sul - UFRGS. Porto Alegre, RS, Brazil, 44 pp (in Portuguese).

Bonotto, D. M., and L. Caprioglio, 2002, Radon in groundwaters from Guarany aquifer, South America: environmental and exploration implications. Applied Radiation and Isotopes 57(6): 931–940. doi: 10.1016/S0969-8043(02)00230-0

Bonotto, D. M., and J. L. N. Lima, 2006, ^{210}Pb-derived chronology in sediment cores evidencing the anthropogenic occupation history at Corumbataí River basin, Brazil. Environmental Geology 50 (4): 595–611. doi: 10.1007/s00254-006-0235-z

Bonotto, D. M., and R. García-Tenorio, 2014, A comparative evaluation of the CF:CS and CRS models in ^{210}Pb chronological studies applied to hydrographic basins in Brazil. Applied Radiation and Isotopes 92: 58–72. doi: 10.1016/j.apradiso.2014.06.012

Bonotto, D. M., K. Y. M. Almeida, and S. S. Sieber, 2005, Sedimentation rates in the Corumbataí River basin, Brazil, derived from ^{210}Pb measurements. In: E. Des Walling, and A. J. Horowitz, (Eds.). Sediment Budgets: v.1; Wallingford: IAHS Press - International Association of Hydrological Sciences. p. 294–302.

Casagrande, M. F. S., and D. M. Bonotto, 2018, The use of γ-rays by HPGe detector to assess the gross alpha and beta activities in waters. Applied Radiation and Isotopes 137: 1–11. doi: 10.1016/j.apradiso.2018.02.027

Cazotti, R. I., A. C. F. Gomes, M. R. L. Nascimento, and A. A. Mozeto, 2006, Isotopic geochronology (^{210}Pb and ^{226}Ra) of limnic sediments: determination of sedimentation velocities and rates, and ages. In: A. A. Mozeto, G. A. Umbuzeiro, and W. F. Jardim, (Eds.). Methods of sampling, physicochemical analysis and biological and ecotoxicological assays of freshwater sediments; São Carlos: Cubo Publishers. p. 37–39 (in Portuguese).

El-Daoushy, F., 1988, A summary on the lead-210 cycle in nature and related applications in Scandinavia. Environment International 14: 305–319. doi: 10.1016/0160-4120(88)90008-6

Faure, G., 1998, Principles and applications of geochemistry: 2nd ed.; Upper Saddle River, NJ: Prentice-Hall, 600 pp.

French, P., 1993, Post-industrial pollutant levels in contemporary Severn Estuary intertidal sediments, compared to pre-industrial. Marine Pollution Bulletin 26: 30–35. doi: 10.1016/0025-326X(93)90594-A

Fúlfaro, V. J., W. L. Ponçano, and C. A. Ciantelli Jr, 1979, The Itanhaém plain (SP). In: Proceedings of the II Regional Symposium of Geology, SBG (Brazilian Geological Society): Rio Claro, SP, Brazil, 15–18 November 1979; v. 1, p. 279–290 (in Portuguese).

García-Orellana, J., and M. García-Léon, 2002, An easy method to determine ^{210}Po and ^{210}Pb by alpha spectrometry in marine environmental samples. Applied Radiation and Isotopes, 56: 633–636. doi: 10.1016/S0969-8043(01)00261-5

Ivanovich, M., and R. S. Harmon, 1992, Uranium-series Disequilibrium: applications to environmental problems: 2nd ed.; New York: Oxford Science, 910 pp.

Kenny, S. P., 2013, The feasibility of using vanadium and nickel to track oil spills in coastal environments. MS Dissertation. Louisiana State University - LSU. Baton Rouge, LA, USA, 138 pp.

Kiehl, E. J., 1977, Interpretation of the soils properties. Monograph. São Paulo University - ESALQ-USP. Piracicaba, SP, Brazil, 237 pp (in Portuguese).

Knoll, G. F., 1989, Radiation detection and measurement: 2nd ed.; New York: John Wiley & Sons, 848 pp.

Kotarba, A., E. Lokas, and P. Wachniew, 2002, ^{210}Pb dating of young Holocene sediments in high-mountains lakes of the Tatra mountains. Geochronometria, 21: 73–78.

Krishnaswami, S., D. Lal, J. M. Martin, and M. Meybeck, 1971, Geochronology of lake sediments. Earth and Planetary Science Letters, 11: 407–414. doi: 10.1016/0012-821X(71)90202-0

Lima, J. L. N., 2000, Pluvial and fluvial hydrochemistry in the Corumbataí River Basin (SP) and relationships with the use of Pb-210 as a geochronometer. PhD Thesis. São Paulo State University - UNESP. Rio Claro, SP, Brazil, 150 pp (in Portuguese).

Loppi, S., F. Riccobono, Z. H. Zhang, S. Savic, D. Ivanov, and S. A. Piritsos, 2003, Lichens as biomonitors of uranium in the Balkan area. Environmental Pollution 125: 277–280. doi: 10.1016/S0269-7491(03)00057-5

Lorenzoni, W. C., 2019, Study of volatile nickel and vanadium compounds in virgin and aged petroleum cement. MS Dissertation. Federal University of Santa Maria - UFSM. Santa Maria, RS, Brazil, 75 pp (in Portuguese).

Matamet, F. R. M., 2013, Use of ^{210}Pb in the chronology of chromium contamination in sediments from Bagres stream, Franca region (SP). PhD Thesis. São Paulo State University - UNESP. Rio Claro, SP, Brazil, 113 pp (in Portuguese).

Nery, J. R. C., 2009, Determination of the sedimentation rate at the Amazon River mouth using ^{210}Pb as a geochronometer. PhD Thesis. São Paulo State University - UNESP. Rio Claro, SP, Brazil, 156 pp (in Portuguese).

Nery, J. R. C., and D. M. Bonotto, 2022, The constant flux and constant sedimentation (CF:CS) ^{210}Pb chronological method applied to determine sedimentation rates at Amazon River watershed, Brazil. Journal of South American Earth Sciences 114: 103715. doi: 10.1016/j.jsames.2022.103715

Riccomini, C., 1989, Continental rift of southeast of Brazil. PhD Thesis. USP-São Paulo University - USP. São Paulo, SP, Brazil, 319 pp (in Portuguese).

Riccomini, C., L. G. Sant'Anna, and A. L. Ferrari, 2004, Geological evolution of the continental rift of southeastern Brazil. In: V. Mantesso-Neto, A. Bartorelli, C. Carneiro, and B. B. Brito-Neves (Eds.). Geology of the South American continent; São Paulo: Beca Publishers. chapter: XXIII, p. 383–406 (in Portuguese).

Sabaris, T. P. P., 2010, The Pb-210 geochronological method applied to the study of the sedimentation rate in a portion of the Atibaia River basin (SP). PhD Thesis. São Paulo State University - UNESP. Rio Claro, SP, Brazil, 152 pp (in Portuguese).

Sallun, A. E. M., and H. N. Diniz, 2016, Natural anomaly of barium, fluorine and sulfur in sedimentary rocks of Tremembé Formation, Taubaté Basin (SP, Brazil) [Anomalia natural de bário, flúor e enxofre em rochas sedimentares da Formação Tremembé, Bacia de Taubaté (SP)]: Geociências / Geosciences, 35 (1): 31–46 (in Portuguese).

Sharma, R., L. R. Gardner, W. S. Moore, and M. S. Bollinger, 1987, Sedimentation and bioturbation in a salt marsh as revealed by ^{210}Pb, ^{137}Cs and ^{7}Be studies. Limnology and Oceanography, 32: 149–162. doi: 10.4319/lo.1987.32.2.0313

Vidal, A. C., F. L. Fernandes, and C. H. Kiang, 2004, Sandstones distribution at Taubaté basin (SP) [Distribuição dos Arenitos na Bacia de Taubaté - SP]: Geociências / Geosciences, 23(1/2): 55–66 (in Portuguese).

BONOTTO D.M.: conception, design and supervision of the study, support for field and analytical steps for data acquisition, data interpretation and final version of the manuscript; **MASSARI J.P.:** field work for the sediment core sampling, data interpretation and first draft version of the manuscript.

Received on July 19, 2022 / Accepted on September 30, 2022